

# Interaction of nucleus reuniens and entorhinal cortex projections in hippocampal field CA1 of the rat

M. J. Dolleman-van der Weel<sup>1,2</sup> · F. H. Lopes da Silva<sup>2,3</sup> · M. P. Witter<sup>4</sup>

Received: 31 May 2016 / Accepted: 14 December 2016 / Published online: 22 December 2016  
© Springer-Verlag Berlin Heidelberg 2016

**Abstract** The nucleus reuniens (RE) and entorhinal cortex (EC) provide monosynaptic excitatory inputs to the apical dendrites of pyramidal cells and to interneurons with dendrites in stratum lacunosum moleculare (LM) of hippocampal field CA1. However, whether the RE and EC inputs interact at the cellular level is unknown. In this electrophysiological *in vivo* study, low-frequency stimulation was used to selectively activate each projection at its origin; field excitatory postsynaptic potentials (fEPSPs) were recorded in CA1. We applied (1) paired pulses to RE or EC, (2) combined paired pulses to RE and EC, and (3) simultaneously paired pulses to RE/EC. The main findings are that: (a) stimulation of either RE- or EC-evoked subthreshold fEPSPs, displaying paired pulse facilitation (PPF), (b) subthreshold fEPSPs evoked by combined stimulation did not display heterosynaptic PPF, and (c) simultaneous stimulation of RE/EC resulted in enhanced subthreshold fEPSPs in proximal LM displaying a nonlinear interaction. CSD analyses of RE/EC-evoked depth profiles revealed a nonlinear enlargement of the ‘LM sink-radiatum source’ configuration and the appearance of an

additional small sink–source pair close to stratum pyramidale, likely reflecting (peri)somatic inhibition. The nonlinear interaction between both inputs indicates that RE and EC axons form synapses, at least partly, onto the same dendritic compartments of CA1 pyramidal cells. We propose that low-frequency activation of the RE-CA1 input facilitates the entorhinal-hippocampal dialogue, and may synchronize the neocortical-hippocampal slow oscillation which is relevant for hippocampal-dependent memory consolidation.

**Keywords** Electrophysiology · Nonlinear summation · Slow oscillation · Synchronization · Memory consolidation · Thalamo–hippocampal interactions

## Introduction

Neural processing in the hippocampus and anatomically related cortices is crucial for learning and memory (Wang and Morris 2010). Activity of neurons in hippocampal field CA1 is generally considered to reflect the convergence of input from CA3 in stratum radiatum and direct EC-CA1 input in stratum lacunosum moleculare (LM; Brun et al. 2002; Remondes and Schuman 2002, 2003). Field CA1 is, however, also targeted by an excitatory subcortical input that arises from the ventral thalamic midline nucleus reuniens (RE), of which the terminal distribution of axons in LM overlaps with the terminations of the direct EC-CA1 projection (Herkenham 1978; Wouterlood et al. 1990; Dolleman-van der Weel et al. 1994; Vertes et al. 2006). In the rat, both RE and EC inputs affect the level of hippocampal excitability by targeting pyramidal cells as well as several types of local interneurons with a dendritic tree in LM (Wouterlood et al. 1990; Colbert and Levy 1992;

✉ M. P. Witter  
menno.witter@ntnu.no

<sup>1</sup> Department of Anatomy and Neurosciences, VU University Medical Center, 1081 BT Amsterdam, The Netherlands

<sup>2</sup> Center for Neuroscience, Swammerdam Institute for Life Sciences, University of Amsterdam, 1098 XH Amsterdam, The Netherlands

<sup>3</sup> Department of Bioengineering, Instituto Superior Técnico, Lisbon Technical University, 1049-001 Lisbon, Portugal

<sup>4</sup> Kavli Institute for Systems Neuroscience and Centre for Neural Computation, MTFs, Norwegian University of Science and Technology (NTNU), Postboks 8905, 7491 Trondheim, Norway

Desmond et al. 1994; Empson and Heinemann 1995; Levy et al. 1995; Dolleman-van der Weel et al. 1997; Dolleman-van der Weel and Witter 2000; Bokor et al. 2002; Klausberger 2009). Surprisingly, the overlap of RE and EC projections in CA1 and its relevance for hippocampal functioning has received little attention.

Recent studies have indicated the importance of RE for cognitive processes, such as behavioural flexibility, strategy shifting, inhibitory response control, associative learning, memory consolidation, working memory, fear memory, memory generalization, goal-directed navigation, and executive behaviours (Dolleman-van der Weel et al. 2009; Davoodi et al. 2011; Eleore et al. 2011; Hembrook et al. 2011; Kincheski et al. 2012; Loureiro et al. 2012; Cholvin et al. 2013; Hallock et al. 2013; Prasad et al. 2013, 2016; Varela et al. 2014; Wheeler et al. 2013; Xu and Südhof 2013; Duan et al. 2015; Griffin 2015; Ito et al. 2015; Layfield et al. 2015; Anderson et al. 2016). This variety of memory-related behaviours has also been associated with the interplay between the medial prefrontal cortex (mPFC) and the hippocampus (Jin and Maren 2015). The mPFC receives a dense hippocampal input, but lacks a direct return projection to the hippocampus (Sesack et al. 1989; Jay and Witter 1991; Hoover and Vertes 2007). Since RE is reciprocally connected with mPFC (Vertes 2002; Vertes et al. 2006), the partially collateralized RE projections to CA1 and mPFC (Hoover and Vertes 2012; Varela et al. 2014), taken together with a closed RE-CA1-subiculum-RE circuit (Dolleman-van der Weel et al. 1997), have led to the notion that RE is an important link between mPFC and the hippocampus. Cognitive alterations resulting from experimental manipulations of RE (i.e., lesions, reversible inactivation, and optogenetic stimulation) support the idea that, instead of specifically affecting the functioning of either the mPFC or hippocampus, RE is mainly involved in orchestrating the flow of hippocampal-mPFC information, likely by modulating the coupling between both structures (Di Prisco and Vertes 2006; Saalman 2014; Cassel and Pereira de Vasconcelos 2015; Ito et al. 2015; Pereira de Vasconcelos and Cassel 2015). The EC has also been shown to play a role in various cognitive tasks (e.g., Skelton and McNamara 1992; Sybirska et al. 2000; Remondes and Schuman 2004; Brun et al. 2008; Deshmukh and Knierim 2011; Suh et al. 2011; Wilson et al. 2013; Chao et al. 2016; Anderson et al. 2016), and both RE and EC appear to be involved in the consolidation of hippocampal-dependent memories (Remondes and Schuman 2004; Loureiro et al. 2012). Moreover, Xu and Südhof (2013) have proposed that the cooperativity between RE-CA1 and EC-CA1 input may reduce the threshold for synaptic plasticity, and thus for the incorporation of entorhinal-transmitted neocortical information

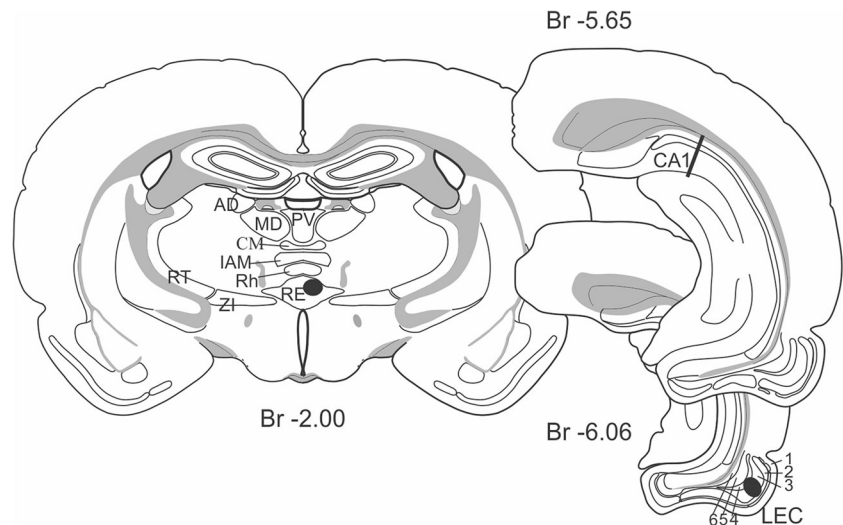
in hippocampal memory representation and subsequent long-term storage.

As yet, the function of the RE input in hippocampal field CA1 is not fully understood. In particular, a possible interaction of the RE-CA1 and EC-CA1 pathways in LM has never been investigated. In the present study, we, therefore, addressed whether an interaction of RE and EC projections in CA1 occurs, and its functional relevance. An important prerequisite to examine the convergence of RE-CA1 and EC-CA1 inputs is to be able to selectively activate each system. This has been achieved in this acute *in vivo* study in which we stimulated the RE-CA1 and lateral EC-CA1 projections at their respective origins, and recorded depth profiles of field potentials in CA1. Because both the RE and lateral EC inputs appear most excitable during low-frequency activation or slow oscillations (<1 Hz) (Dolleman-van der Weel et al. 1997; Schall et al. 2008), we recorded depth profiles of field potentials in CA1 elicited by a range of low-frequency stimulation protocols. Current-source-density (CSD) analyses of the evoked depth profiles were performed to provide the sites of synaptic activity in CA1. Our results show that co-activation of RE and EC inputs yields a major nonlinear enhancement of the elicited field potentials and associated sink in proximal LM. This indicates that RE and EC axons form synapses, at least partly, onto the same dendritic compartments of pyramidal cells. Moreover, the obtained CSD profiles reveal an additional (peri)somatic inhibition evoked by simultaneous activation of the RE-CA1 and EC-CA1 projections. We conclude that the influence of RE and EC on neural processing in CA1 is strongly enhanced during coincident low-frequency activation of both inputs. We further suggest that the RE-CA1 input has the ability to synchronize the hippocampal and mPFC slow oscillations, which is important for memory consolidation.

## Materials and methods

We used 15 male Wistar rats (Harlan CPB, Zeist, The Netherlands), weighing 275–375 g. Under halothane anesthesia, the trachea was intubated. The rat was then placed in a stereotaxic apparatus and throughout the experiment artificially ventilated by a mixture of O<sub>2</sub> and N<sub>2</sub>O with 1% halothane. Body temperature was maintained using a heating pad. All experiments were carried out according to the guidelines laid down by the European Communities Council Directive (1986), and with the approval of the local Animal Experimentation Committee of the VU University Medical Centre, Amsterdam. All efforts were made to minimize any suffering and the number of animals used.

**Fig. 1** Schematic representation of the stimulation sites in RE and lateral EC (black dots) and the recording site in CA1 (black line). Figures are modified from Swanson (1998). RE nucleus reuniens, AD anterodorsal nucleus, MD mediodorsal nucleus, PV paraventricular nucleus, CM central medial nucleus, IAM interanteromedial nucleus, Rh rhomboid nucleus, ZI zona incerta, RT reticular nucleus, CA1 hippocampal field CA1, LEC lateral entorhinal cortex, 1–6 EC layers 1–6, Br bregma



Based on anatomical observations (Dolleman-van der Weel et al. 1994), the stimulation sites in RE and lateral EC (layer III) were chosen, such that the corresponding terminations would be optimally placed to overlap with the recording sites in stratum LM of CA1 (see Fig. 1). Stereotaxic coordinates were derived from Paxinos and Watson (1986). They were zeroed at bregma (Br), the midline of the midsagittal sinus, and the dura surface. Stimulation electrodes in RE were lowered into position at an angle of 15 degrees in the coronal plane using the following coordinates: Br.,  $-1.80$  mm; lateral (L) 2.0 mm; and ventral (V), 7.0 mm. The coordinates for stimulation electrodes in lateral EC were: Br.,  $-5.8$  mm; L, 6.0 mm; and V, 6.1 mm, and for recording electrodes in CA1: Br.,  $-5.6$  mm, L, 4.3 mm; and V, 1.6–3.1 mm. To prevent the exposed tissue from dehydration, the brain surface was covered with warm paraffin oil.

### Stimulation protocols and data acquisition

The RE-CA1 input elicits larger amplitude responses during stimulation at low frequencies (0.1–2 Hz) than at theta frequency (4–10 Hz) (Dolleman-van der Weel et al. 1997), and the lateral EC-CA1 projection also shows greater excitability during slow oscillations ( $<1$  Hz) than during oscillations in the theta range (Schall et al. 2008). Therefore, we choose low-frequency ( $<1$  Hz) stimulation of RE and EC inputs to investigate their combined influence on neural excitability in CA1. Electrical stimulation of RE and EC was performed using an electrode array of three stainless steel wires (diameter 60  $\mu$ m, insulated except the tip) that were obliquely arranged. This electrode array was positioned in RE, covering the rostro-caudal extent of the nucleus; within the EC, it was predominantly aimed at layer III. To optimize evoked responses, stimulation of RE

and EC was varied between different pairs of the electrode array. The standard stimulation protocol consisted of monopolar paired pulses of equal strength and duration [0.2 ms; interpulse interval (IPI) 100 ms, unless stated otherwise; intensity 350–650  $\mu$ A; 0.13 Hz]. The first stimulus of a pair is referred to as the conditioning pulse, the second one as the test pulse. Protocols for combined stimulation of the RE-CA1 and EC-CA1 projections consisted of an RE-EC stimulation sequence (IPI 50 ms; occasionally IPI 25 ms) and/or an RE-EC-RE-EC sequence of stimuli (IPI range 25–100 ms), occasionally vice versa starting with EC stimulation. Simultaneous RE/EC stimulation consisted of the standard paired pulses (IPI 100 ms) applied to each input structure. Whenever response latencies differed, the RE and EC stimulations were timed, such that the peaks of the conditioning RE- and EC-evoked fEPSPs coincided. For nearby inputs onto neocortical pyramidal cells, Nettleton and Spain (2000) have reported that two synaptic events, occurring within a 5 ms time window, were integrated as coinciding events. Therefore, we occasionally timed RE and EC stimulations, such that the peaks of their respective responses had a 4 ms delay.

CA1 depth profiles of fEPSPs were obtained using an array of six equally spaced stainless steel wires (diameter 60  $\mu$ m, insulated except the tip; inter-electrode distance 250  $\mu$ m;  $n = 12$ ), arranged in the same plane. To obtain depth profiles for CSD analyses ( $n = 3$ ), we used a specially constructed probe of 18 electrodes (stainless steel wires, diameter 60  $\mu$ m, insulated except the tip; electrode heart-to-heart distance, 100  $\mu$ m, along the sloping side of the probe, see Fig. 4f), tightly glued together in the same plane. Both types of recording probes were cut at an angle of approximately 30° (Dolleman-van der Weel et al. 1997). They covered the depth of CA1 from the deep cortical layer/white matter down to the hippocampal fissure, or just

into the dentate gyrus. The shape of these electrode arrays allowed for recordings approximately perpendicular to the curved longitudinal axis of the hippocampus, i.e., corresponding to the orientation of the apical dendrites of the pyramidal cells (see Figs. 1, 4f). Evoked field potentials were amplified and digitized by way of an interface (CED 1401 plus) connected to a personal computer. They were sampled at a rate of 5000/s, averaged ( $n = 32$ ), and stored for off-line analysis.

### Off-line analysis

Characteristics of CA1 fEPSPs were studied in laminar depth profiles. Response latencies were defined as the time from the onset of the stimulus artefact to the peak of the conditioning response. Paired pulse facilitation (PPF) was expressed as the ratio between test response amplitude/conditioning response amplitude. PPF was calculated for field potentials recorded in stratum LM, representing the summed active synaptic processes. Statistical analyses of heterosynaptic PPF, evoked by combined RE and EC stimulation and recorded with a six-electrode probe, were done with an ANOVA; significance was set at  $p < 0.05$ . In addition, the amplitude of conditioning responses in LM elicited by simultaneous RE/EC activation was compared with responses elicited by single RE or EC stimulation.

One-dimensional CSD analyses (Freeman and Nicholson 1975) show estimates of the local trans-membrane currents, resulting from the excitatory and inhibitory synaptic inputs. We made a two-step CSD analysis of the recorded CA1 depth profiles according to the formula:

$$\text{CSD}(h) = \left[ \frac{\phi(h - \Delta h) - 2 * \phi(h) + \phi(h + \Delta h)}{(\Delta h)^2} \right] * \sigma_h$$

in which  $\text{CSD}(h)$  = current-source density at depth  $h$ ,  $\phi(h)$  = averaged field potential at depth  $h$ ,  $\Delta h$  = depth interval (100  $\mu\text{m}$ ), and  $\sigma_h$  = conductivity in the direction of the track, here assumed to be constant. Spontaneous activity (i.e., recorded 0–50 ms immediately before the first stimulus) was averaged and subtracted from each of the recorded traces. Smoothing of the depth profile was performed using a moving averaging window consisting of five points with weights: +1, 0, -2, 0, +1. Since the value of  $\sigma_h$  was not determined, CSDs ( $\text{mV}/\text{mm}^2$ ) were in arbitrary units.

We calculated the CSDs of CA1 depth profiles recorded following (1) stimulation of RE, (2) stimulation of EC, and (3) simultaneous RE/EC stimulation. We also calculated the CSD of a theoretical depth profile which consisted of the algebraic sum of the single RE- and EC-evoked depth profiles, i.e., a depth profile which was to be expected in case RE and EC inputs activated independently different

subsets of CA1 neurons. In principle, comparison of the theoretical CSD with the experimental CSD reveals whether or not RE and EC inputs interact at the cellular level.

### Histological control

At the end of the experiment, under deep anesthesia, the stimulation and recording electrodes were marked by lesions (three pulses of 1 mA anodal current) that resulted in a blue spot, due to the potassium ferrocyanide in the fixative (see below), occasionally with a hole in the centre of the lesion. The rat was decapitated, and the brain removed and stored for 3 days in 4% paraformaldehyde and 0.05% glutaraldehyde in 0.1 M phosphate buffer with potassium ferrocyanide. The tissue was cryoprotected in 2% dimethylsulfoxide and 20% glycerin, and cut on a freezing microtome in 40  $\mu\text{m}$ -thick coronal sections. Subsequently, the sections were Nissl-stained and examined for verification of electrode placements.

## Results

### CA1 responses to paired pulse stimulation of RE and EC

Stimulation of either RE or lateral EC at locations as represented in Fig. 1 resulted in field potentials in CA1. The elicited depth profiles showed a large negative-going deflection in the recordings from LM. In stratum radiatum, the deflections were positive-going, and gradually decreased towards the alvear surface (Fig. 2a–c). RE- and EC-evoked field potentials displayed peak latencies ranging from 14 to 21 ms, varying with the relative positions of stimulating and recording electrodes. A common feature of RE-CA1 and EC-CA1 responses was the consistent lack of a population spike at all stimulation intensities used. These results are in accordance with the previous findings (Colbert and Levy 1992; Empson and Heinemann 1995; Dolleman-van der Weel et al. 1997; Morales et al. 2007). Inadvertent co-stimulation of EC layer II cells elicited a large amplitude field potential, often with a population spike, in the dentate gyrus (DG; Fig. 2b, arrows) at slightly shorter latency than the co-evoked CA1 response. Stimulation of deeper EC layers (III/IV/V; Köhler 1985) resulted in eight cases in two negative-going deflections in LM, of which the first short latency peak (Fig. 2c, white arrow) did not reverse polarity in stratum radiatum, whereas the second LM peak did reverse (Fig. 2c, black arrow). In contrast to the monosynaptic input from the rostral RE (Dolleman-van der Weel et al. 1997), we have to consider the possibility that EC-evoked responses can result from activation of multiple pathways, i.e., monosynaptic EC-CA1,

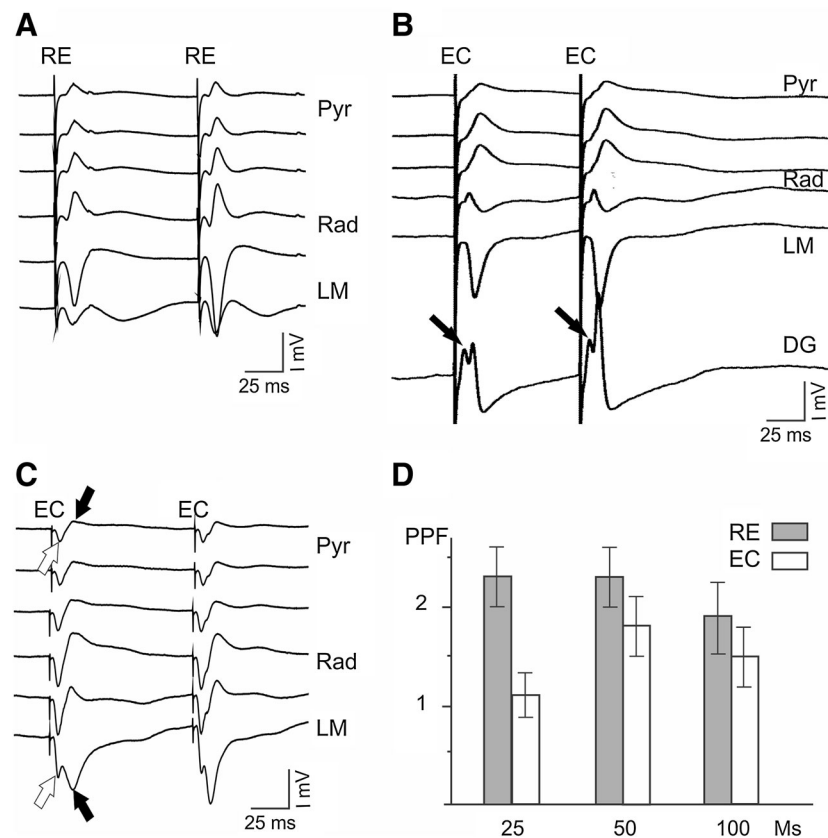


**Fig. 2** CA1 responses to stimulation of reuniens (RE) and the lateral entorhinal cortex (EC), and paired pulse facilitation (PPF). **a–c** Subthreshold fEPSPs were evoked by stimulation of RE (**a**) or EC (**b, c**); RE- or EC-induced field potentials were negative-going in LM and positive-going in radiatum. **b** EC stimulation of layers II/III evoked field potentials in CA1 and in DG, the latter with a population spike (*arrows*) and at slightly shorter peak latency than the CA1 response. The DG field potential, recorded rather close to the cell layer, was positive-going. **c** When the stimulation electrode array covered the EC layers III/IV/V, the CA1 response displayed two

negative-going waves in LM; the first one (*open arrows*) did not reverse polarity, whereas the second one (*black arrows*) reversed to a positive-going wave near the LM/radiatum border. **d** PPF was calculated for 25, 50, and 100 ms interpulse intervals (IPI). Both RE and EC stimulation resulted in robust PPF at IPIs of 50 and 100 ms. Yet, whereas at 25 ms IPI, RE-induced PPF was just as robust as at 50 ms, EC-induced PPF was hardly, if at all, noticeable. *Pyr* stratum pyramidale, *Rad* stratum radiatum, *LM* stratum lacunosum moleculare, *DG* dentate gyrus

disynaptic EC-CA3-CA1, and/or tri-synaptic EC-DG-CA3-CA1 inputs. Yet, in our recordings, di- or tri-synaptic CA1 responses can be ruled out, because (1) the latency difference between the evoked field potentials in DG and CA1 was very small, and thus, a tri-synaptic input in CA1 is unlikely and (2) the depth profile evoked by di- or tri-synaptic input to CA1, both via the Schaffer collaterals, is known to be opposite (i.e., positive-going in LM, negative-going in radiatum) to that of the actually recorded depth profiles in CA1 (i.e., negative-going in LM, positive-going in radiatum; Colbert and Levy 1992). Therefore, we conclude that the recorded CA1 responses were monosynaptically elicited by direct EC-CA1 input. In addition, entorhinal fibres have been reported to reach CA1 via the alvear pathway. On the way to their terminal field in LM, these alvear EC axons make synaptic contacts in the strata oriens, pyramidale, and radiatum with pyramidal cells and, to a much higher extent, with inhibitory neurons (Deller

et al. 1996; Takács et al. 2011). Hence, it is possible that the early negative deflections, recorded throughout the depth of the CA1 profile, may reflect EC input via the alvear pathway.

We next analyzed whether RE- and EC-evoked local field potentials displayed paired pulse facilitation (PPF) (Fig. 2d). Usually, low-intensity stimulation of RE- and EC-evoked small and weak responses, particularly in case of the EC-evoked field potentials in LM. Therefore, we applied high-intensity paired pulses (0.13 Hz; IPI range 25–50–100 ms), which resulted in reliably measurable RE- and EC-evoked responses (Dolleman-van der Weel et al. 1997; Di Prisco and Vertes 2006; Eleore et al. 2011; Aksoy-Aksel and Manahan-Vaughan 2013). RE-induced PPF was robust at the standard 100 ms IPI (PPF  $1.9 \pm 0.4$ ,  $n = 15$ ), and even stronger at shorter intervals (IPI 25 and 50 ms; PPF  $2.3 \pm 0.3$ ,  $n = 6$ ). This was also found for the EC-induced PPF both at IPI 100 ms (PPF  $1.5 \pm 0.3$ ,  $n = 15$ ) and IPI

50 ms (PPF  $1.8 \pm 0.3$ ,  $n = 5$ ). However, at IPI 25 ms, EC-induced PPF was hardly noticeable (PPF  $1.1 \pm 0.2$ ,  $n = 4$ ). These findings are in agreement with those reported in the previous studies (Sloviter 1991; Leung et al. 1995; Dolleman-van der Weel et al. 1997; Eleore et al. 2011; Ito and Schuman 2012; Gonzalez et al. 2016).

### Combined stimulation of RE and EC

In subsequent experiments, we used various stimulation protocols to examine whether the responses to RE- and EC activation showed interaction or were independent. First, since there was a pronounced PPF of both RE- and EC-evoked responses at a 50 ms interval, we used this stimulation protocol as reference to examine the effects of heterosynaptic paired pulse stimulation. A representative example of such stimulation shows that a conditioning stimulus applied to RE did not significantly affect the amplitude of the field potential in LM evoked by a following EC test stimulus (Fig. 3a; mean peak amplitudes of an EC-elicited LM conditioning response  $1.31 \pm 0.32$  mV, and a heterosynaptic EC-elicited LM test response  $1.36 \pm 0.31$  mV,  $n = 9$ ;  $F_{(1,16)} = 0.078$ ,  $p = 0.783$ , n.s.). Second, in some instances, we applied a conditioning stimulus to EC and a test stimulus to RE, which did not affect the RE-evoked LM response (mean peak amplitudes of an RE-elicited LM conditioning response  $0.98 \pm 0.43$  mV, and a heterosynaptic RE-elicited LM test response  $1.03 \pm 0.49$  mV,  $n = 4$ ;  $F_{(1,6)} = 0.017$ ,  $p = 0.899$ , n.s.; not illustrated, but see also Fig. 3d). Even at a shorter interval of 25 ms, RE stimulation did not affect the amplitude of the EC test response in LM (Fig. 3b); the reversed stimulation sequence (i.e., an EC conditioning pulse followed by an RE test pulse; Fig. 3c) yielded similar results. In addition, we employed RE-EC-RE-EC stimulation sequences. As shown in Fig. 3d–e, RE- and EC-induced PPF was comparable to PPF evoked by paired pulse stimulation of RE or EC separately. Thus, in line with earlier reports, indicating that PPF is specific to the set of afferents excited by the first stimulus (Creager et al. 1980; Grover and Teyler 1992), heterosynaptic PPF between RE and EC, or vice versa, was not observed. Third, we applied paired pulses (IPI 100 ms) to RE/EC simultaneously (Fig. 3f). Compared to an RE- or EC-elicited LM conditioning response (mean peak amplitude  $0.76 \pm 0.22$  and  $0.86 \pm 0.11$  mV, respectively;  $n = 6$ ), the RE/EC-elicited LM conditioning response (mean peak amplitude  $1.53 \pm 0.26$  mV,  $n = 6$ ) was significantly enlarged (RE/EC versus RE stimulation alone,  $F_{(1,10)} = 7.264$ ,  $p = 0.022$ ; RE/EC versus EC stimulation alone,  $F_{(1,10)} = 6.920$ ,  $p = 0.025$ ). Compared to an RE- or EC-elicited LM test response (mean peak amplitude  $1.37 \pm 0.52$  and  $1.45 \pm 0.35$  mV, respectively), the

enlargement of the RE/EC-elicited LM test response (mean peak amplitude  $2.14 \pm 0.30$  mV) just did not reach significance (RE/EC versus RE stimulation alone,  $F_{(1,10)} = 4.357$ ,  $p = 0.063$ , trend; RE/EC versus EC stimulation alone,  $F_{(1,10)} = 4.359$ ,  $p = 0.063$ , trend). Because depth profiles recorded with an 18 electrode array yielded more detail, the interaction between both inputs underlying the RE/EC-evoked enlargement of the fEPSP in LM will be described below while examining the CSDs.

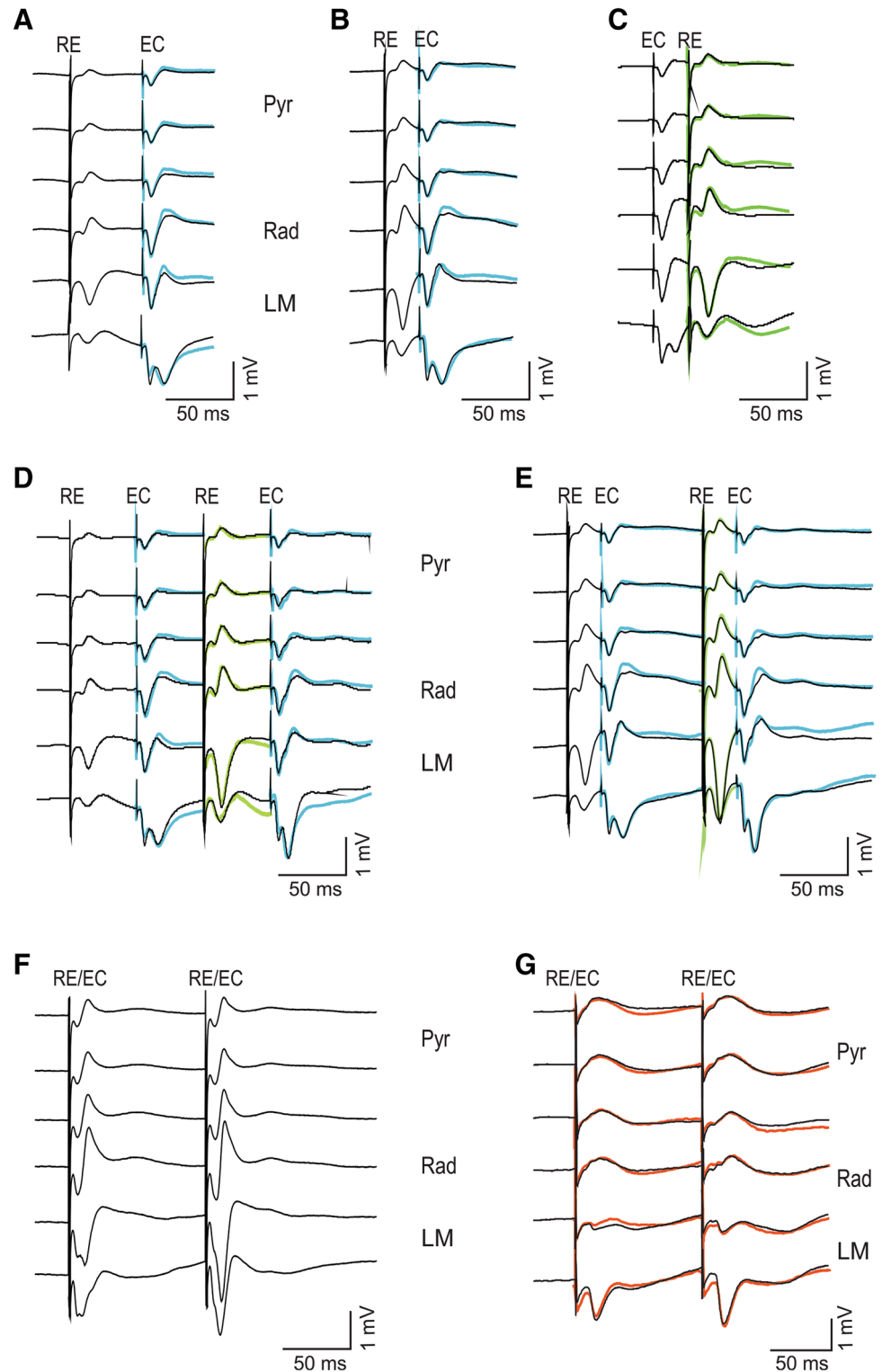
Since RE- and EC-evoked response latencies could be different, we timed the stimuli, so that the position of the initial response peaks in LM coincided. In addition, based on observations of Nettleton and Spain (2000) that nearby inputs occurring within a 5 ms time window may be integrated as coinciding events, we also recorded RE/EC-evoked responses of which the initial LM peaks had a 4 ms latency difference. Figure 3g shows superimposed the RE/EC-evoked response obtained with appropriately timed stimuli (in black) and those for which a delay of 4 ms was maintained (in red). These CA1 responses were very similar, which is in agreement with the report of Nettleton and Spain (2000).

Yet, despite the markedly increased amplitude of LM field potentials, simultaneous stimulation of RE/EC never elicited population spikes. This inability of RE and EC to drive pyramidal cells under all test conditions is likely due to inhibitory influences mediated by both inputs (see “Discussion”).

### CSD analyses

Using an 18-electrode probe, we next investigated whether the superposition of RE and EC inputs would yield responses that may be interpreted as resulting from a summation process in case of independent inputs, or whether signs of an interaction at the cellular level could be found. Accordingly, we compared the responses evoked by simultaneous RE/EC stimulation with the corresponding RE- and EC-evoked responses added algebraically [i.e., (RE + EC)]. In general, following simultaneous RE/EC stimulation the CSD analyses from three different rats showed an enhancement of the evoked field potentials in LM and the associated LM sink. Because RE/EC stimulation appeared to affect the CA1 response in a complex way throughout the depth of the profile, we describe the observed effects in some detail. The results of a representative experiment are shown in Figs. 4 and 5, illustrating the single RE-, single EC-, simultaneous RE/EC- and theoretical (RE + EC)-elicited CA1 depth profiles, and CSDs, respectively. The EC stimulation electrode was positioned in layers III/IV, and the RE stimulation electrode was placed in the mid rostro-caudal part of the nucleus, corresponding to the EC and RE stimulation sites

**Fig. 3** Absence of heterosynaptic facilitation following combined stimulation of RE and EC (a–f show recordings from one rat; g shows recordings from a different rat). **a** Conditioning pulse to RE followed by a test pulse to EC (IPI 50 ms) did not result in heterosynaptic facilitation, as shown by comparison with an EC conditioning response (superimposed *blue traces*). **b** Similar results were obtained at 25 ms IPI. **c** Vice versa, a conditioning pulse to EC followed by an RE test pulse (IPI 25 ms) had no effect on the RE-evoked field potential, as compared with an RE conditioning pulse (*green traces*). **d, e** Combining paired pulses to RE and EC at various intervals also had no effect on their respective field potentials or PPF, as indicated by comparison with their separately evoked responses (RE *green traces*; EC *blue traces*). **f** Simultaneous paired pulse stimulation of RE/EC (IPI 100 ms) resulted in a markedly enlarged field potential in LM. **g** Applying paired pulses to RE and EC, either simultaneously (*black traces*) or with a 4 ms delay (*red traces*) between RE and EC stimulation, yielded similar responses



represented in Fig. 1. The recording 18-electrode array was positioned in the dorsal part of the intermediate CA1, perpendicular to the curved axis of the CA1 field (see Fig. 4f). The most superficial electrode was located in the white matter and the deepest electrode just across the

fissure in the dentate gyrus. Compared to the RE- and EC-elicited depth profiles (Fig. 4a, b), simultaneous stimulation of RE/EC (Fig. 4c) yielded a conspicuous effect: namely, an enlargement of the field potentials in LM, especially of the deflections close to radiatum, i.e., in

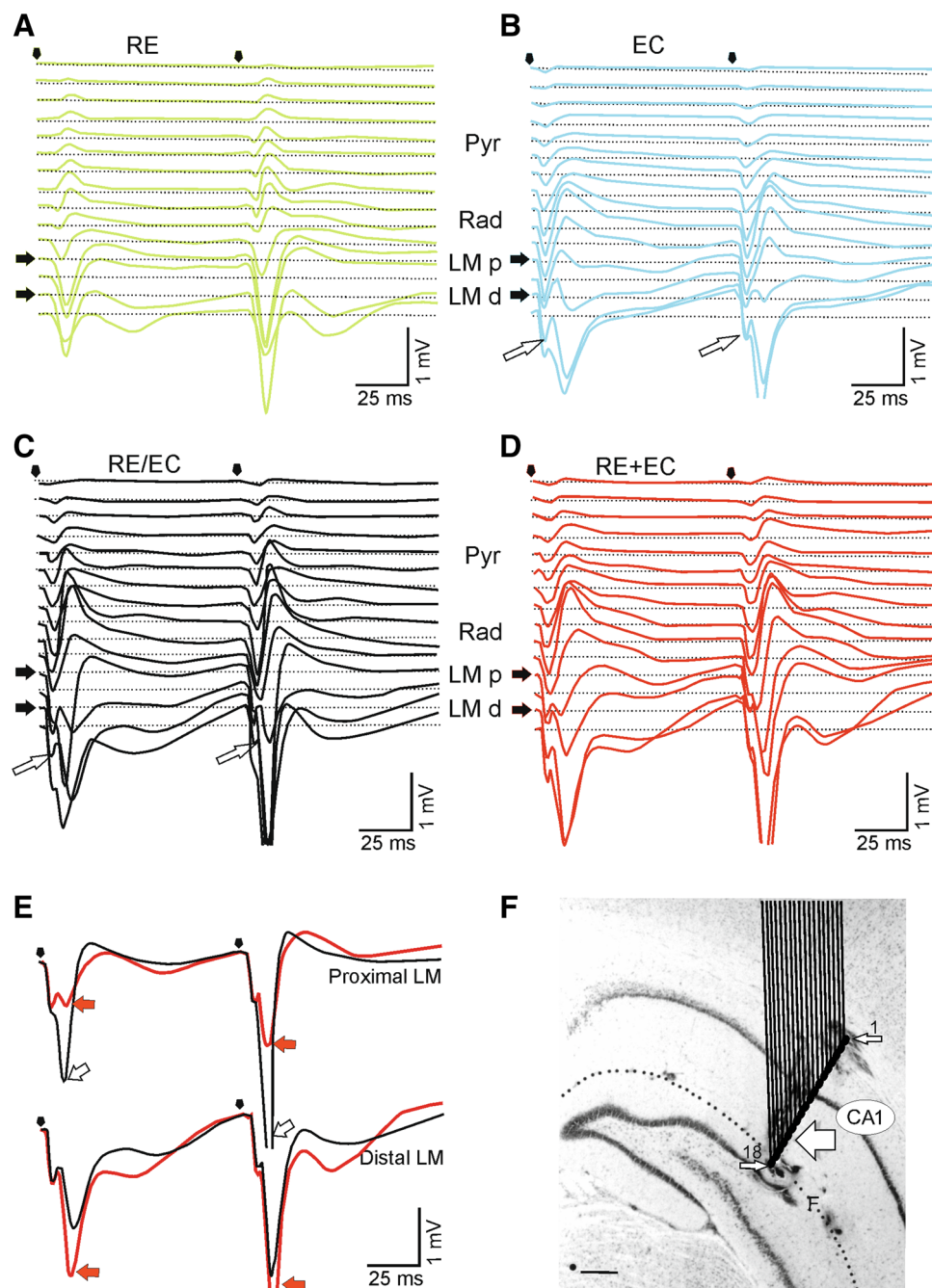


**Fig. 4** Depths profiles of evoked field potentials in CA1; recordings from electrodes 4–18 are illustrated. **a** RE-elicited depth profile has large negative-going potentials in LM and positive-going ones in radiatum. **b** In this case, the EC-elicited depth profile shows two negative-going LM field potentials; the first, small one does not reverse polarity (*open arrows*), whereas the second, larger one reverses polarity close to the LM/radiatum border. **c** Experimental RE/EC depth profile, elicited by simultaneous stimulation, displays (1) a small negative potential (*open arrow*), similar to that in the EC profile, and (2) a robust enhancement of the LM field potential. Due to a large overlap of traces in the depth profile this is difficult to visualize in this plot; therefore, see LM traces in **e**. **d** Summated (theoretical) RE + EC depth profile is different from the experimentally induced one (see also overlays in **e**). **e** Peak amplitude of the

experimental RE/EC-elicited field potential (*black trace, open arrows*) in proximal LM is much larger than the theoretical one (*red trace, red arrows*). In contrast, in distal LM, the peak amplitude of the theoretical RE + EC-elicited field potential (*red trace, red arrows*) is larger than the experimental RE/EC-induced one (*black trace*). **f** Micrograph showing the position of the 18-electrode recording probe in the dorsal part of the intermediate CA1, placed perpendicular to the hippocampal lamina. The most superficial electrode (1, *small white arrow*) and the deepest electrode (18, *small white arrow*) were marked by a lesion/blue spot. Electrode 1 was located in the white matter; electrode 18 was located just across the fissure (**f**) in the dentate gyrus. *Large white arrow* indicates the LM/radiatum border. Scale bar 500 μm. Test response field potentials in LM are truncated in **b–e**. *LMp* proximal LM, *LMd* distal LM



proximal LM (LMp). In this way, the response to simultaneous RE/EC stimulation contrasted not only with the response to RE and EC separately, but also with the theoretical (RE + EC)-evoked depth profile (Fig. 4d). This latter effect can be appreciated better in Fig. 4e [red = theoretical (RE + EC); black = experimental RE/EC]. We have previously shown that RE and EC display homogeneously distributed projections in LM (Dolleman-van der Weel et al. 1994; see Fig. 6e). These observations are in agreement with earlier publications (e.g., Steward 1976; Witter et al. 1988; Wouterlood et al. 1990). Although we cannot entirely exclude some variation in specificity or efficacy, as hinted to in recent publications concerning EC projections to CA1 (e.g., Kitamura et al. 2014; Basu et al. 2016), it is unlikely that an (anatomical) uneven distribution of RE and/or EC fibres in LM underlies the predominant effect of coinciding RE/EC input in proximal LM. To further clarify this finding, we made CSD analyses of the different depth profiles (Fig. 5a–d). Whereas the RE CSD showed a clear LM sink–radiatum source configuration (Fig. 5a), the EC CSD showed multiple sinks and sources, which is likely due to a recruitment of EC–CA1 fibres in both perforant path and alveus (Fig. 5b). Comparison of the experimental RE/EC CSD (Fig. 5c), and the simply algebraically added (RE + EC) CSD profiles (Fig. 5d) revealed marked differences that are indicative for a non-linear interaction, and where this interaction may take place. Specifically, a very strong sink in proximal LM was observed in the RE/EC CSD but not in that of the simple summation model (Fig. 5e, LMp). In the experimental RE/EC CSD profile, in distal LM (Fig. 5c, LMd), we recognized a sink–source–sink sequence that was rather similar to the sink–source–sink sequence in the single EC CSD (Fig. 5b, LMd, 5F lowest superimposed traces), but the large distal LM sink is smaller in the experimental RE/EC CSD than in the theoretical one (Fig. 5e, LMd). Taken together, this suggests that the influence of RE input on the EC-elicited field potentials is more prominent in proximal versus distal LM (Fig. 5e; see also Fig. 6, at 14 ms). Another remarkable feature of the RE/EC CSD was a small sink–source pair (Fig. 5c, yellow boxed area) close to stratum pyramidale, not seen in the RE, EC, and (RE + EC) CSDs (Fig. 5a, b, d, f; boxed areas). Similar small sink–source pairs close to the pyramidal cell level were detected in the CSDs from all three rats. This additional effect of RE/EC stimulation presumably represents an inhibitory input at the (peri)somatic level (see discussion). In contrast, the small early sinks and sources in strata pyramidale and radiatum in the EC CSD (Fig. 5b, thick black lines), possibly reflecting alvear EC input, seemed unaffected by simultaneous RE/EC stimulation (Fig. 5c). Because a presumed alvear input was quite variable in our experiments, and the early pyramidal and radiatum sink–

source pairs at 7 ms emerged just from the background, rendering them rather fragile, this precludes a detailed interpretation at this time. The sink in proximal radiatum (Fig. 5b, circled areas) was also unaffected by RE/EC input [Fig. 5b, c, f, middle superimposed EC (blue) and RE/EC (black) traces]. Although this sink is rather substantial, as yet its origin, and whether this is an active or passive sink, is not clear. More data are needed for a detailed interpretation of the underlying mechanism(s). Thus, we focus here on the more robust effects of RE/EC stimulation.

To further clarify the RE/EC interactions, we examined more in detail the CSD profiles at 6.5, 14, and 17 ms, resulting from the conditioning pulse (Fig. 6). These three timepoints represent approximately the peak latencies of the early, small sinks–sources pairs and of the later, large sinks, and sources in the CSD depth profiles of Fig. 5. First, at 6.5 ms, there were no sinks and sources noticeable in the RE CSD profile, and thus, the single EC- and theoretical (RE + EC) CSD depth profiles were largely similar, except for some enhancement of the early small sink–source pair in LM (Fig. 6, lines 11–9). This was suggestive for an unexpected, yet minor contribution of RE to the RE/EC-evoked early synaptic response in LM (see also “Discussion”). Second, at 14 ms, a large LM sink (towards radiatum) was most pronounced for the RE/EC case, suggesting that the main site of interaction between RE and EC takes place on dendritic compartments of CA1 cells in proximal LM. Thus, coinciding RE input appears, at least partly, to ‘overrule’ an EC-induced inhibition onto the apical dendrites of the pyramidal cells. This inhibitory effect is likely represented by the occurrence of the LM source, of which the decay phase (at 14 ms) seems to mask the onset of the EC-elicited LM sink (see Fig. 5b). Third, at 17 ms, comparison of the experimental RE/EC and the theoretical (RE + EC) CSDs revealed that summation throughout the depth of the CA1 profile was mainly linear, except for minor broadening of the LM sink towards radiatum, indicating ongoing interaction in the apical dendrites in proximal LM.

## Discussion

The present findings form a strong indication that RE and EC axons actually converge, at least partly, onto the same apical dendritic compartment of CA1 pyramidal cells. Following simultaneous low-frequency stimulation of both inputs the elicited CA1 response shows (1) a major non-linear enhancement of subthreshold RE- and EC-evoked fEPSPs in proximal LM and (2) a small sink–source pair at the pyramidal cell level, likely reflecting an additional (peri)somatic inhibition.

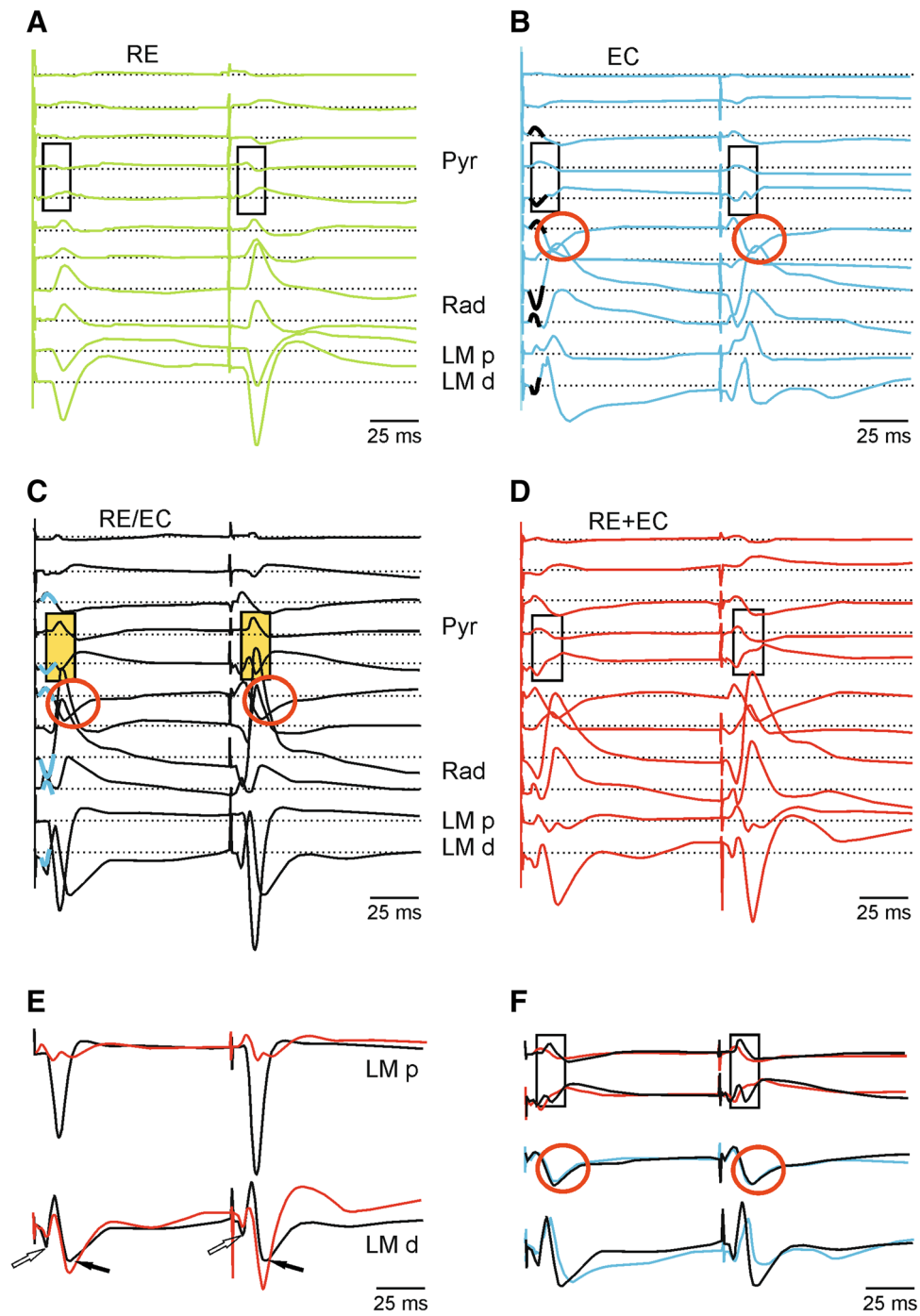


**Fig. 5** CSDs, corresponding to the depth profiles shown in Fig. 4 (sinks are *downward*, sources *upward*, in arbitrary units). **a** RE CSD profile displays a clear ‘LM sink-radiatum source’ configuration. **b** EC CSD shows a series of early small sink–source pairs (*thick black lines*) throughout the depth profile, followed by larger sinks and sources with a longer time course. **c** Experimental RE/EC CSD displays a markedly enlarged ‘LM sink-radiatum source’, but also maintains some of the characteristics of the EC CSDs, i.e., (1) the series of early sinks and sources (*thick blue lines*), (2) a sink in proximal radiatum (*red circles*; for comparison see circled areas in **b**, **c**, and **f** middle superimposed traces), and (3) the sink–source–sink sequence in distal LM (LMd, **b**, **c**; **f** lowest superimposed traces), respectively. There was also a small sink–source configuration close to stratum pyramidale (*yellow box*), which was not observed in any of the other CSDs (*boxed areas in a*, **b**, **d**, and **f** upper superimposed traces). **d** Theoretical, summated (RE + EC) CSD profile was different from the experimental RE/EC CSD profile, especially in proximal LM (LMp). **e** Superimposed traces of the experimental RE/EC CSD (*black lines*) and the theoretical RE + EC CSD (*red lines*) show the substantial enlargement of the experimentally recorded sink in proximal LM (LMp). The experimental first small sink in distal LM (*black line/open arrows*, LMd) is slightly larger than the theoretical one (*red line*, LMd), while the experimental second LM sink (*black arrows*) is smaller than the summated one. **f** *Upper* two traces show superimposed the RE/EC CSD (*black*) and the summated RE + EC CSD (*red*) at the pyramidal cell level, clearly revealing the appearance of a small sink–source pair (*boxed area*) in the experimental CSD (*black*). Middle superimposed traces show the similarity of the radiatum sink (*circled areas*) in the EC CSD (*blue*) and in the experimental RE/EC CSD (*black*). The lowest superimposed traces show the similarity of the dLM sink–source–sink sequence in the EC (*blue*) and RE/EC (*black*) CSDs. They also reveal that compared to the EC CSD (*blue*), the RE/EC CSD (*black*) shows (1) a slight enhancement of the early small sink, (2) a shorter duration of the experimental source (in *black*), and (3) some ‘disinhibition’ of the late LM sink in the test response of the RE/EC CSD (*black*)

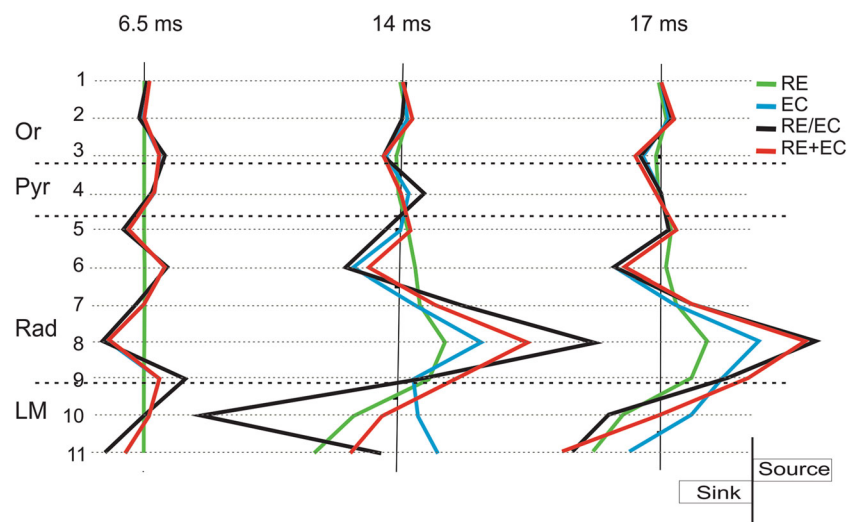


**Fig. 6** Detailed cross section of the CSD profiles shown in Fig. 5 ( $t = 6.5$  ms,  $t = 14$  ms, and  $t = 17$  ms correspond to time points of the conditioning response; sinks and sources are in arbitrary units). At 6.5 ms, there are no noticeable RE-elicited sink/source pairs, and thus, a simple *straight line* is shown (*green*). The RE/EC-elicited experimental response (*black*) and theoretically (RE + EC) evoked response (*red*) are shown; the EC-elicited response is not shown, because it coincides with the *red line*. Simultaneous input from RE/EC (*black*) yielded a small enlargement of the early LM sink and associated source at the LM-radiatum border. At  $t = 14$  ms, the RE/

The analysis of inputs to CA1 shows a strong focus on the excitatory projections from EC and CA3, and how they might interact with each other as well as with local connectivity, mainly originating from the many classes of interneurons (Klausberger and Somogyi 2008; Klausberger 2009). Entorhinal axons in LM form asymmetrical synaptic contacts on spines and shafts of CA1 cells (Desmond et al. 1994), and it is generally accepted that the EC and CA3 inputs converge onto single pyramidal cells (Kajiwara et al. 2008). RE-CA1 axons also form asymmetrical synapses on spines and dendritic shafts in LM (Wouterlood et al. 1990). Preliminary ultrastructural data have confirmed that RE forms synapses on spines and shafts of identified (i.e., intracellularly labeled) CA1 pyramidal cells (own unpublished observations). Previous light microscopical data support a convergence of RE as well as EC axons onto the apical dendrites of CA1 cells (Dolleman-van der Weel et al. 1994). Here, we provide the first data indicating that RE and EC inputs indeed converge, at least partly, onto single pyramidal neurons.

Many (in vitro) electrophysiological studies have examined the interplay between CA3–CA1 and direct EC–CA1 inputs stimulated via the Schaffer collaterals in radiatum and perforant path fibres in LM, respectively, and the spatial distribution of activated synapses (e.g., Judge and Hasselmo 2004; Ang et al. 2005; Dudman et al. 2007; Izumi and Zorumski 2008; Takahashi and Magee 2009;

EC input resulted in a nonlinear summation of evoked potentials throughout the depth of the profile. Most obvious is the major increase in the amplitudes of the ‘LM sink-radiatum source’ (see *thin lines* 10 and 8, respectively), and the shift of the LM sink towards radiatum. In addition, a small source appeared at the pyramidal cell level (see *thin line* 4). At 17 ms, the experimental RE/EC (*black*) and theoretical (RE + EC) (*red*) CSD profiles are largely similar, except for some minor broadening of the experimental LM sink towards radiatum, indicating ongoing interaction in proximal LM

Pissadaki et al. 2010; McQuiston 2010). Yet, the contribution of inadvertently co-activated RE axons in LM was not taken into consideration. The present *in vivo* results are the first to shed light on the individual contributions of RE and EC to a coinciding RE/EC input in CA1. This implies that, in case of *in vitro* stimulation of axons in radiatum and LM, the observed effects of CA3 and EC interactions on transmission in CA1 may in fact reflect, at least partly, the converging inputs from RE and EC, together with CA3 input. Such reported effects are: (1) changes in spiking activity of pyramidal cells (Remondes and Schuman 2002; Takahashi and Magee 2009; Pissadaki et al. 2010); (2) modification of long-term synaptic changes in both inputs (Remondes and Schuman 2003; Judge and Hasselmo 2004; Dudman et al. 2007); (3) gating of Schaffer collaterals input by preceding LM stimulation (McQuiston 2010) and, vice versa, gating of EC input by preceding Schaffer collaterals stimulation (Ang et al. 2005). Overall, these differential effects appeared dependent on timing, spatial synaptic arrangement, and stimulation frequencies of LM axons and Schaffer collaterals.

There is evidence that convergent inputs onto the dendrites of CA1 pyramidal cells result in a nonlinear summation of evoked potentials (Wei et al. 2001; Poirazi et al. 2003; Liang 2006). Gasparini and Magee (2006) demonstrated that the response patterns of CA1 pyramidal cells depend on whether the converging inputs are either asynchronous and distributed in space, resulting in linear processing, or are synchronous and spatially clustered, resulting in nonlinear processing. The latter form of integration is in line with the present results, thus suggesting that RE-CA1 and EC-CA1 inputs converge on the same dendritic branch of a pyramidal cell.

Synaptic summation in CA1 cells is also controlled by GABAergic inputs (Enoki et al. 2001). In general, an inhibitory control mechanism is necessary to coordinate the activities of numerous principal cells. At least 21 classes of functionally different interneurons in CA1 allow for the flexibility with which pyramidal cells can enhance their computational abilities. Thirteen of these interneuron types have dendrites in LM and thus, in theory, can be activated by RE and EC inputs (Klausberger and Somogyi 2008; Klausberger 2009; Roux and Buzsáki 2015). As schematically summarized in Fig. 7, the excitatory RE and EC innervation of several classes of interneurons provides potentially a powerful inhibitory influence covering the entire depth of field CA1. RE has been shown to drive vertical oriens/alveus (O/A) cells, mediating feedforward perisomatic inhibition of CA1 cells (Lacaille et al. 1987; Samulack et al. 1993; McBain et al. 1994; Dolleman-van der Weel et al. 1997). Furthermore, RE drives interneurons in distal radiatum that fire only in response to low-frequency (0.1–2 Hz)

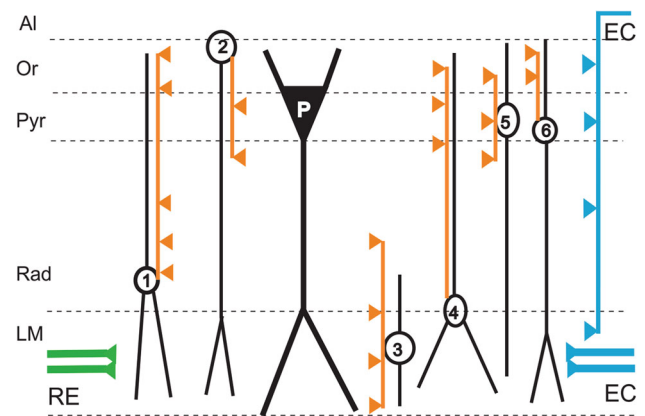


**Fig. 7** Schematic representation of excitatory RE and EC inputs in CA1 onto pyramidal cells and interneurons (modified from Klausberger and Somogyi 2008). The CA1 pyramidal cell (in *thick black*, *white P*) receives presumed inhibitory synaptic inputs represented by the *orange triangles*, and excitatory inputs corresponding to the *blue* and *green triangles*. The inhibitory inputs are presented alongside the axons (in *orange*) of the corresponding interneurons and not next to the pyramidal cell for clarity. RE (*green*) and EC input (via perforant path and alveus; *blue*) innervate the apical dendrites of CA1 pyramidal cells as well as several subclasses of interneurons with a dendritic tree (*black*) in LM (for clarity these excitatory inputs are not presented next to their dendritic targets). RE innervates presumed Schaffer collaterals associated cells (1) which are thought to inhibit pyramidal cells and other (unidentified) interneurons, and vertical oriens/alveus cells (2), mediating feedforward perisomatic inhibition of CA1 cells. EC innervates LM-neurogliaform cells (3), providing feedforward inhibition of pyramidal cells as well as other interneurons in LM, and parvalbumine-positive basket cells (5) and chandelier or axo-axonic cells (6), providing feedforward somatic and axonal inhibition, respectively. Synaptic targets of alvear EC input (*blue*) are pyramidal cells, and to a larger extent, unspecified interneurons (Takács et al. 2011). The present results indicate that RE and EC inputs converge onto the same dendritic branch of a pyramidal cell in proximal LM, and presumably also on a specific set of interneurons, possibly a subclass of basket cells located at the LM/radiatum border (4), which provide (peri)somatic inhibition of CA1 cells. *Al* alveus, *Or* stratum oriens, *Pyr* stratum pyramidale, *Rad* stratum radiatum, *LM* stratum lacunosum moleculare, *RE* nucleus reuniens, *EC* entorhinal cortex

stimulation of RE, but are silent during stimulation at theta (4–10 Hz) frequencies (Dolleman-van der Weel et al. 1997). These interneurons are presumably Schaffer collaterals associated with cholecystokinin-positive (CCK<sup>+</sup>) cells which innervate pyramidal cells and other classes of interneurons, as well as each other (Nunzi et al. 1985; Acsády et al. 1996; Gulyás et al. 1996; Vida et al. 1998; Somogyi and Klausberger 2005; Klausberger 2009; Chamberland and Topolnik 2012). The excitatory RE innervation of GABAergic cells in CA1 has also been confirmed at the ultrastructural level (Dolleman-van der Weel and Witter 2000). EC axons in LM innervate parvalbumine-positive (PV<sup>+</sup>) basket cells and chandelier or axo-axonic cells, providing powerful feedforward somatic and axonal inhibition, respectively (Somogyi et al. 1983; Li et al. 1992; Kiss et al. 1996). In

addition, the presently described small sink–source pair at the pyramidal cell level in the RE/EC CSD (see Fig. 5c) may reflect an RE/EC-mediated (peri)somatic inhibition. Because RE and EC do not provide an excitatory input in stratum pyramidale, we propose that this small sink–source pair represents an active (i.e., inhibitory) source and a passive sink, probably originating from RE/EC-induced activation of a subclass of CCK/vasoactive intestinal polypeptide (VIP)-positive (CCK<sup>+</sup>/VIP<sup>+</sup>) basket cells located at the LM/radiatum border (Klausberger and Somogyi 2008; Kajiwara et al. 2008). These CCK<sup>+</sup>/VIP<sup>+</sup> basket cells exert a powerful feedforward inhibitory influence at the (peri)somatic level, which effectively suppresses the generation of action potentials in CA1 cells (Freund and Katona 2007). EC-activated PV<sup>+</sup> basket cells and presumed RE/EC-activated CCK<sup>+</sup>/VIP<sup>+</sup> basket cells are thought to have different functions, such as distinct contributions to network oscillations and/or targeting different subtypes of pyramidal cells (e.g., Klausberger et al. 2005; Klausberger and Somogyi 2008; Lee et al. 2014; Donato et al. 2015; Roux and Buzsáki 2015). Although this awaits further investigation, such an RE/EC-evoked activation of CCK<sup>+</sup>/VIP<sup>+</sup> basket cells can exert a strong inhibitory influence on the output abilities of CA1 cells. Furthermore, in LM, a variety of interneurons is supposed to gate the entorhinal-hippocampal dialogue (Cagnagna 2011). Price et al. (2005, 2008) have shown that LM-neurogliaform (LM-NG) cells are monosynaptically activated by stimulation of EC fibres in LM in a slice preparation. They suggested that, next to innervating other LM interneurons, LM-NG cells might be specialized for shunting inhibition of EC-CA1 input. In line with this idea, we propose that the sink–source–sink sequence in LM in the EC CSD (see Fig. 5b) consists of (1) a small early sink, presumably reflecting the excitatory EC input onto LM-NG cells. Because these interneurons have all their dendrites and a very compact axonal plexus in LM, they may generate currents strong enough to be detected in a CSD. (2) The succeeding LM source may then reflect the (EC-mediated) feed forward inhibitory input of LM-NG cells onto the apical dendrites of the pyramidal cells (Price et al. 2008), and (3) the large LM sink, of which the onset likely summates with the preceding (inhibitory) source, represents the direct EC excitatory input onto the CA1 cell dendrites in LM. So far, there is no evidence for RE innervation of LM-NG cells and/or other subclasses of LM interneurons. Yet, the presently observed small enhancement of the early sink in LM in the RE/EC CSD (see Fig. 6 at 6.5 ms) seems at least suggestive for a minor RE input on presumed LM-NG cells. Since these effects are small, a presumed RE innervation/activation of LM-NG cells

requires further confirmation, both at the electrophysiological (e.g., pairwise recordings) as well as at the anatomical (e.g., intracellular labeling or ultrastructural) level.

Overall, the present data reveal that simultaneous RE/EC activation resulted in an increased excitation level of the pyramidal cell dendrites, predominantly in proximal LM. This indicates that convergence of EC- and RE inputs onto the same dendritic compartments of CA1 pyramidal cells partly ‘overrules’ the ‘on-the-path’ shunting inhibition (Koch et al. 1983; Hao et al. 2009) exerted by EC-activated LM-NG cells. Such an enhanced dendritic excitation level in the apical tuft of pyramidal cells can lead to the generation of dendritic spikes which, reliant on the presence/modulation of voltage dependent channels and the level of synaptic inhibition (Jarski et al. 2005; Ibarz et al. 2006; Hao et al. 2009), may propagate towards the CA1 soma, initiating action potentials. Although it is possible that dendritic spikes were overlooked, all aforementioned RE- and EC-mediated inhibitory influences together (see Fig. 7) offer an adequate explanation for the absence of dendritic spikes and the consistent lack of pyramidal cell firing in our recordings.

### Functional relevance

Regarding the interactions of RE and EC input in CA1, there are two important questions: (1) whether coincident low-frequency input of the RE-CA1 and the lateral EC-CA1 pathways is a natural occurring phenomenon and (2) what the functional importance of such interactions might be. As yet, there are no studies available, showing that during low-frequency oscillations (as in slow-wave-sleep or during immobility), the RE-CA1 and the EC-CA1 projections are simultaneously active. In fact, the coincidence of RE and EC inputs in hippocampal field CA1 has never been examined. Nonetheless, Xu and Südhof (2013) have suggested that the cooperative activation of RE-CA1 and EC-CA1 synapses may reduce the threshold for synaptic plasticity, thereby facilitating transmission in CA1 and subsequent memory consolidation, a process that is improved by slow oscillations (Heib et al. 2013). In line with this idea, the present data show at least that coinciding low-frequency activation of the RE and EC inputs results in a strongly enhanced excitation level of the CA1 cell apical dendrites in LM.

Recent studies in freely moving rats have shed some light on the physiological properties of RE neurons (Janowski et al. 2014, 2015). Next to a relatively small percentage of cells with diverse spatial properties, the vast majority of RE neurons (~64%) appeared to be low-frequency firing cells without spatial properties, of which approximately 17% fired only at frequencies below 1 Hz

(Jankowski et al. 2014). Thus, low-frequency stimulation of RE, as applied in this study, appears to mimic the physiological properties of a large group of RE neurons. Previously, we have stimulated the RE-CA1 projection at frequencies ranging from 0.13 to 10 Hz, and found that low-frequency (0.13–2 Hz) activation of RE evokes the largest LM field potentials (Dolleman-van der Weel et al. 1997). Therefore, we suggest that the RE-CA1 input shows enhanced synaptic excitability during slow oscillations. Since interneurons play important roles in the regulation of oscillations (Jonas et al. 2004; Somogyi and Klausberger 2005; Klausberger 2009), it is noteworthy that low-frequency ( $\leq 2$  Hz) RE input is also able to drive interneurons in distal radiatum (Dolleman-van der Weel et al. 1997) that inhibit both pyramidal cells and other inhibitory interneurons. Driving these particular radiatum interneurons may thus provide a possible mechanism for RE to impose a slow oscillation on CA1 cells, as previously reported by Zhang et al. (2012). RE-induced oscillatory activity in CA1 may be in synchrony with slow oscillations in mPFC. This idea is supported by the fact that the RE-CA1 projecting neurons receive input from mPFC (Vertes et al. 2007). In addition, a small percentage of these RE neurons project via collateralized axons to CA1 as well as back to mPFC, and thus have the potential to directly synchronize the activity in both target areas (Hoover and Vertes 2012; Varela et al. 2014). Moreover, paired pulse stimulation at 0.1 Hz of the RE-mPFC projection has been shown to exert pronounced excitatory effects in mPFC, displaying strong PPF similar to RE-induced PPF in CA1 (Dolleman-van der Weel et al. 1997; Di Prisco and Vertes 2006; Eleore et al. 2011; present study). Taken together, these findings are supportive for a pivotal role of RE in synchronizing the activities in hippocampus and mPFC. Such synchronous slow oscillations, occurring during slow-wave sleep, are crucially important for the consolidation of hippocampal-dependent memories (Sirota et al. 2003; Sirota and Buzsáki 2005; Marshall et al. 2006; Wolansky et al. 2006; Isomura et al. 2006; Wang and Morris 2010; Mölle and Born 2011; Heib et al. 2013; Binder et al. 2014). It has also been assumed that hippocampal theta oscillations may play a role in memory processes. Recently, causal evidence was presented for the role of rapid eye movement (REM) sleep theta rhythm in contextual memory consolidation (Boyce et al. 2016). Therefore, it is timely to investigate the interaction of coinciding RE-CA1 and EC-CA1 inputs with hippocampal theta oscillations in future studies.

A growing number of behavioural studies have provided evidence that RE is indeed involved in cognitive functions, most likely by coordinating neuronal activities in hippocampus and mPFC (Dolleman-van der Weel et al. 2009; Davoodi et al. 2011; Eleore et al. 2011; Hembrook et al. 2011; Loureiro et al. 2012; Prasad et al. 2013;

Cholvin et al. 2013; Hallock et al. 2013; Xu and Südhof 2013; Saalman 2014; Bobal and Savage 2015; Ito et al. 2015; Layfield et al. 2015; Prasad et al. 2016). Because mPFC lacks a direct return projection to the hippocampus (Sesack et al. 1989; Jay and Witter 1991), RE might relay mPFC-processed information back to the hippocampus as part of a closed CA1-mPFC-RE-CA1 circuit (Vertes et al. 2007; Xu and Südhof 2013). In addition, mPFC-processed information can be transmitted to CA1 via the lateral EC (Preston and Eichenbaum 2013; Takehara-Nishiuchi 2014; Chao et al. 2016), an area that can also be influenced by RE input (Wouterlood 1991; Dolleman-van der Weel and Witter 1996; Zhang and Bertram 2002; Wouterlood et al. 2008).

In summary, viewed in the context discussed above, we propose that low-frequency RE input in CA1 is potentially important for the synchronization of hippocampal and mPFC slow oscillations. Whether synchronization actually takes place and, however, has to be tested quantitatively. Furthermore, the present electrophysiological data strongly suggest that, by directly and indirectly facilitating the EC-CA1 input during slow oscillations, RE can contribute to the dialogue between hippocampus and mPFC which is of crucial importance for the consolidation of hippocampal-dependent memories.

**Acknowledgements** This work was supported by NWA Grant 90-20 from the Graduate School for Neurosciences Amsterdam. We thank A.J.A. Juta for helping with the calculation of the CSDs.

## References

- Acsady L, Gorcs TJ, Freund TF (1996) Different populations of vasoactive intestinal polypeptide-immunoreactive interneurons are specialized to control pyramidal cells or interneurons in the hippocampus. *Neuroscience* 73:317–334
- Aksoy-Aksel A, Manahan-Vaughan D (2013) The temporoammonic input to the hippocampal CA1 region displays different synaptic plasticity compared to the Schaffer collateral input in vivo: significance for synaptic information processing. *Front Syn Neurosci* 5:5. doi:10.3389/fnsyn.2013.00005
- Anderson MC, Bunce JG, Barbas H (2016) Prefrontal-hippocampal pathways underlying inhibitory control over memory. *Neurobiol Learn Mem* 134 PtA:145–161
- Ang CW, Carlson GC, Coulter DA (2005) Hippocampal CA1 circuitry dynamically gates direct cortical inputs preferentially at theta frequencies. *J Neurosci* 25:9567–9580
- Basu J, Zaremba JD, Cheunh SK, Hitti FL, Zemelman BV, Losonezy A, Siegelbaum SA (2016) Gating of hippocampal activity, plasticity, and memory by entorhinal cortex long-range inhibition. *Science* 351:aaa5694 doi:10.1126/science.aaa5694
- Binder S, Rawohl J, Born J, Marshall L (2014) Transcranial slow oscillation stimulation during NREM sleep enhances acquisition of the radial maze task and modulates cortical network activity in rats. *Front Behav Neurosci*. doi:10.3389/fnbeh.2013.00220
- Bobal MG, Savage LM (2015) The role of ventral midline thalamus in cholinergic-based recovery in the amnesic rat. *Neuroscience* 285:260–268

- Bokor H, Csaki A, Kocsis K, Kiss J (2002) Cellular architecture of the nucleus reuniens thalami and its putative aspartatergic/glutamatergic projection to the hippocampus and medial septum in the rat. *Eur J Neurosci* 16:1227–1239
- Boyce R, Glasgow SD, Williams S, Adamantidis A (2016) Causal evidence for the role of REM sleep theta rhythm in contextual memory consolidation. *Science* 352:812–816
- Brun VH, Otnass MK, Moiden S, Steffenach HA, Witter MP, Moser MB, Moser EI (2002) Place cells and place recognition maintained by direct entorhinal-hippocampal circuitry. *Science* 296:2243–2246
- Brun VH, Leutgeb S, Wu HQ, Schwarcz R, Witter MP, Moser EI, Moser MB (2008) Impaired spatial representation in CA1 after lesion of direct input from entorhinal cortex. *Neuron* 57:290–302
- Capogna M (2011) Neurogliaform cells and other interneurons of stratum lacunosum-moleculare gate entorhinal-hippocampal dialogue. *J Physiol* 589:1875–1883
- Cassel JC, Pereira de Vasconcelos A (2015) Importance of the ventral midline thalamus in driving hippocampal functions. *Prog Brain Res* 219:145–161
- Chamberland S, Topolnik L (2012) Inhibitory control of hippocampal inhibitory neurons. *Front Neurosci* 6:165. doi:10.3389/fnins.2012.00165
- Chao OY, Huston JP, Li JS, Wang AL, de Souza Silva MA (2016) The medial prefrontal cortex-lateral entorhinal cortex circuit is essential for episodic-like memory and associative object-recognition. *Hippocampus* 26:633–645
- Cholvin T, Loureiro M, Cassel R, Cosquer B, Geiger K, De Sa Nogueira D, Raingard H, Robelin L, Kelche C, Pereira de Vasconcelos A, Cassel JC (2013) The ventral midline thalamus contributes to strategy shifting in a memory task requiring both prefrontal cortical and hippocampal functions. *J Neurosci* 33:8772–8783
- Colbert CM, Levy WB (1992) Electrophysiological and pharmacological characterization of perforant path synapses in CA1: mediation by glutamate receptors. *J Neurophysiol* 68:1–8
- Creager R, Dunwiddie T, Lynch G (1980) Paired-pulse and frequency facilitation in the CA1 region of the in vitro rat hippocampus. *J Physiol* 299:409–424
- Davoodi FG, Motamedi F, Akbari E, Ghanbarian E, Jila B (2011) Effect of reversible inactivation of reuniens nucleus on memory processing in passive avoidance task. *Behav Brain Res* 221:1–6
- Deller T, Adelmann G, Nitsch R, Frotscher M (1996) The alvear pathway of the rat hippocampus. *Cell Tissue Res* 286:293–303
- Deshmukh SS, Knierim JJ (2011) Representation of non-spatial and spatial information in the lateral entorhinal cortex. *Front Behav Neurosci* 5:69. doi:10.3389/fnbeh.2011.00069
- Desmond NL, Scott CA, Jane JA Jr, Levy WB (1994) Ultrastructural identification of entorhinal cortical synapses in CA1 stratum lacunosum-moleculare of the rat. *Hippocampus* 4:594–600
- Di Prisco GV, Vertes RP (2006) Excitatory actions of the ventral midline thalamus (rhomboid/reuniens) on the medial prefrontal cortex in the rat. *Synapse* 60:45–55
- Dolleman-van der Weel MJ, Witter MP (1996) Projections from the nucleus reuniens thalami to the entorhinal cortex, hippocampal field CA1, and the subiculum in the rat arise from different populations of neurons. *J Comp Neurol* 364:637–650
- Dolleman-van der Weel MJ, Witter MP (2000) Nucleus reuniens thalami innervates gamma aminobutyric acid positive cells in hippocampal field CA1 of the rat. *Neurosci Lett* 278:145–148
- Dolleman-van der Weel MJ, Wouterlood FG, Witter MP (1994) Multiple anterograde tracing, combining Phaseolus vulgaris leucoagglutinin with rhodamine- and biotin-conjugated amine. *J Neurosci Methods* 51:9–21
- Dolleman-van der Weel MJ, Lopes da Silva FH, Witter MP (1997) Nucleus reuniens thalami modulates activity in hippocampal field CA1 through excitatory and inhibitory mechanisms. *J Neurosci* 17:5640–5650
- Dolleman-van der Weel MJ, Morris RG, Witter MP (2009) Neurotoxic lesions of the thalamic reuniens or mediodorsal nucleus in rats affect non-mnemonic aspects of watermaze learning. *Brain Struct Funct* 213:329–342
- Donato F, Chowdhury A, Lahr M, Caroni P (2015) Early- and late-born parvalbumine basket cell subpopulations exhibiting distinct regulation and roles in learning. *Neuron* 85:770–786
- Duan AR, Varela C, Zhang Y, Shen Y, Xiong L, Wilson MA, Lisman J (2015) Delta frequency optogenetic stimulation of the thalamic nucleus reuniens is sufficient to produce working memory deficits: relevance to schizophrenia. *Biol Psychiatry* 77:1098–1107
- Dudman JT, Tsay D, Siegelbaum SA (2007) A novel role for synaptic inputs at distal dendrites: instructive signals for hippocampal long-term plasticity. *Neuron* 56:866–879
- Eleore L, López-Ramos JC, Guerra-Narbona R, Delgado-García JM (2011) Role of reuniens nucleus projections to the medial prefrontal cortex and to the hippocampal pyramidal CA1 area in associative learning. *PLoS One* 6:e23538. doi:10.1371/journal.pone.0023538
- Empson RM, Heinemann U (1995) The perforant path projection to hippocampal area CA1 in the rat hippocampal-entorhinal cortex combined slice. *J Physiol* 484:707–720
- Enoki R, Inoue M, Hashimoto Y, Kudo Y, Miyakawa H (2001) GABAergic control of synaptic summation in hippocampal CA1 pyramidal neurons. *Hippocampus* 11:683–689
- Freeman JA, Nicholson C (1975) Experimental optimization of current-source-density techniques for anuram cerebellum. *J Neurophysiol* 38:369–382
- Freund TF, Katona I (2007) Perisomatic inhibition. *Neuron* 56(1):33–42
- Gasparini S, Magee JC (2006) State-dependent dendritic computation in hippocampal CA1 pyramidal neurons. *J Neurosci* 26:2088–2100
- Gonzalez J, Villarreal DM, Morales IS, Derrick BE (2016) Long-term potentiation at temporoammonic path-CA1 synapses in freely moving rats. *Front Neural Circuits* 10:2. doi:10.3389/fncir.2016.00002
- Griffin AL (2015) Role of the thalamic nucleus reuniens in mediating interactions between the hippocampus and medial prefrontal cortex during spatial working memory. *Front Syst Neurosci* 9:29. doi:10.3389/fnsys.201500029
- Grover LM, Teyler TJ (1992) N-methyl-D-aspartate receptor-independent long-term potentiation in area CA1 of rat hippocampus: input-specific induction and preclusion in a non-tetanized pathway. *Neuroscience* 49:7–11
- Gulyás AI, Hajos N, Freund TF (1996) Interneurons containing calretinin are specialized to control other interneurons in the rat hippocampus. *J Neurosci* 16:3397–3411
- Hallock HL, Wang A, Shaw CL, Griffin AL (2013) Transient inactivation of the thalamic nucleus reuniens and rhomboid nucleus produces deficits of a working-memory dependent tactile-visual conditional discrimination task. *Behav Neurosci* 127:860–866
- Hao J, X-d Wang, Dan Y, M-m Poo, X-h Zhang (2009) An arithmetic rule for spatial summation of excitatory and inhibitory inputs in pyramidal neurons. *PNAS* 106:21906–21911
- Heib DPJ, Hoedlmoser K, Anderer P, Zeitlhofer J, Gruber G, Klimesch W, Schabus M (2013) Slow oscillations amplitudes and up-state lengths relate to memory improvement. *PLoS One* 8:e82049. doi:10.1371/journal.pone.0082049
- Hembrook JR, Onos KD, Mair RG (2011) Inactivation of ventral midline thalamus produces selective spatial delayed conditional discrimination impairment in the rat. *Hippocampus* 22:853–860

- Herkenham M (1978) The connections of the nucleus reuniens thalami: evidence for a direct thalamo-hippocampal pathway in the rat. *J Comp Neurol* 177:589–609
- Hoover WB, Vertes RP (2007) Anatomical analysis of afferent projections to the medial prefrontal cortex in the rat. *Brain Struct Funct* 212:149–179
- Hoover WB, Vertes RP (2012) Collateral projections from nucleus reuniens of thalamus to hippocampus and medial prefrontal cortex in the rat: a single and double retrograde fluorescent labeling study. *Brain Struct Funct* 217:191–209
- Ibarz JM, Makarova I, Herreras O (2006) Relation of apical dendritic spikes to output decision in CA1 pyramidal cells during synchronous activation: a computational study. *Eur J Neurosci* 23:1219–1233
- Isomura Y, Sirota A, Ozen S, Montgomery S, Mizuseki K, Henze DA, Buzsáki G (2006) Integration and segregation of activity in entorhinal-hippocampal subregions by neocortical slow oscillations. *Neuron* 52:871–882
- Ito HT, Schuman EM (2012) Functional division of hippocampal area CA1 via modulatory gating of entorhinal cortical inputs. *Hippocampus* 22:372–387
- Ito HT, Zhang S, Witter MP, Moser EI, Moser MB (2015) A prefrontal-thalamo-hippocampal circuit for goal-directed spatial navigation. *Nature* 522:50–55
- Izumi Y, Zorumski CF (2008) Direct cortical inputs erase long-term potentiation at Schaffer collateral synapses. *J Neurosci* 28:9557–9563
- Jankowski MM, Islam MN, Wright NF, Vann SD, Erichsen JT, Aggleton JP, O'Mara SM (2014) Nucleus reuniens of the thalamus contains head direction cells. *Elife*. doi:10.7554/elife.03075
- Jankowski MM, Passecker J, Islam MN, Erichsen JT, Aggleton JP, O'Mara SM (2015) Evidence for spatially-responsive neurons in the rostral thalamus. *Front Behav Neurosci* 9:256. doi:10.3389/fnbeh.2015.00256
- Jarski T, Roxin A, Kath WL, Spruston N (2005) Conditional dendritic spike propagation following distal synaptic activation of hippocampal CA1 pyramidal neurons. *Nat Neurosci* 8:1667–1676
- Jay TM, Witter MP (1991) Distribution of hippocampal and subicular efferents in the prefrontal cortex of the rat studied by means of anterograde transport of Phaseolus vulgaris-leucoagglutinin. *J Comp Neurol* 313:574–586
- Jin J, Maren S (2015) Prefrontal-hippocampal interactions in memory and emotion. *Front Syst Neurosci* 9:170. doi:10.3389/fnsys.2015.00170
- Jonas P, Bischofberger J, Fricker D, Miles R (2004) Interneuron diversity series: fast in, fast out—temporal and spatial signal processing in hippocampal interneurons. *Trends Neurosci* 27:30–40
- Judge SJ, Hasselmo ME (2004) Theta rhythmic stimulation of stratum lacunosum moleculare in rat hippocampus contributes to associative LTP at a phase offset in stratum radiatum. *J Neurophysiol* 92:1615–1624
- Kajiwara R, Wouterlood FG, Sah A, Boekel AJ, Baks-te Bulte LT, Witter MP (2008) Convergence of entorhinal and CA3 inputs onto pyramidal neurons and interneurons in hippocampal area CA1—an anatomical study in the rat. *Hippocampus* 18:266–280
- Kinchski GC, Mota-Ortiz SR, Pavesi E, Canteras NS, Carobrez AP (2012) The dorsolateral periaqueductal gray and its role in mediating fear learning to life threatening events. *PLoS One* 7:e50361. doi:10.1371/journal.pone.0050361
- Kiss J, Buzsáki G, Morrow JS, Glantz SB, Leranath C (1996) Entorhinal cortical innervation of parvalbumin-containing neurons (basket and chandelier cells) in the rat Ammon's horn. *Hippocampus* 6:239–246
- Kitamura T, Pignatelli M, Suh J, Kohara K, Yoshiki A, Abe K, Tonewaga S (2014) Island cells control temporal association memory. *Science* 343:896–901
- Klausberger T (2009) GABAergic interneurons targeting dendrites of pyramidal cells in the CA1 area of the hippocampus. *Eur J Neurosci* 30:947–957
- Klausberger T, Somogyi P (2008) Neuronal diversity and temporal dynamics: the unity of hippocampal circuit operations. *Science* 321:53–57
- Klausberger T et al (2005) Complementary roles of cholecystokinin- and parvalbumin-expressing GABAergic neurons in hippocampal network oscillations. *J Neurosci* 25:9782–9793
- Koch C, Poggio T, Torre V (1983) Nonlinear interactions in a dendritic tree: Localization, timing, and role in information processing. *Proc Natl Acad Sci USA* 80:2799–2802
- Köhler C (1985) A projection from the deep layers of the entorhinal area to the hippocampal formation in the rat. *Neurosci Lett* 56:13–19
- Lacaille J-C, Mueller AI, Kunkel DD, Schwarzkroin PA (1987) Local circuit interactions between oriens/alveus interneurons and CA1 pyramidal cells in hippocampal slices: electrophysiology and morphology. *J Neurosci* 7:1979–1993
- Layfield DM, Patel M, Hallock H, Griffin AL (2015) Inactivation of the nucleus reuniens/rhomboid causes a delay-dependent impairment of spatial working memory. *Neurobiol Learn Mem* 125:163–167
- Lee SH, Marchionni I, Bezaire M, Varga C, Danielson N, Lovett-Barron M, Losonczy A, Soltesz I (2014) Parvalbumin-positive basket cells differentiate among hippocampal pyramidal cells. *Neuron* 82:1129–1144
- Leung LS, Roth L, Canning KJ (1995) Entorhinal inputs to hippocampal CA1 and dentate gyrus in the rat: a current-source-density study. *J Neurophysiol* 73:2392–2403
- Levy WB, Colbert CM, Desmond NL (1995) Another network model bites the dust: entorhinal inputs are no more than weakly excitatory in the hippocampal CA1 region. *Hippocampus* 5:137–140
- Li X-G, Somogyi P, Tepper JM, Buzsáki G (1992) Axonal and dendritic arborization of an intracellularly labelled chandelier cell in the CA1 region of rat hippocampus. *Exp Brain Res* 90:519–525
- Liang CW (2006) One dendritic arbor, two modes of integration. *J Neurosci* 26:6664–6665
- Loureiro M, Colvin T, Lopez J, Merienne N, Latreche A, Cosquer B, Geiger K, Kelche C, Cassel J-C, de Vasconcelos AP (2012) The ventral midline thalamus (reuniens and rhomboid nuclei) contributes to the persistence of spatial memory in rats. *J Neurosci* 32:9947–9959
- Marshall L, Helgadóttir H, Mölle M, Born J (2006) Boosting slow oscillations during sleep potentiates memory. *Nature* 444:610–613
- McBain CJ, DiChiara TJ, Kauer JA (1994) Activation of metabotropic glutamate receptors differentially affects two classes of hippocampal interneurons and potentiates excitatory synaptic transmission. *J Neurosci* 14:4433–4445
- McQuiston AR (2010) Cholinergic modulation of excitatory synaptic input integration in hippocampal CA1. *J Physiol* 588:3727–3742
- Mölle M, Born J (2011) Slow oscillations orchestrating fast oscillations and memory consolidation. *Prog Brain Res* 193:93–110
- Morales GJ, Ramcharan EJ, Sundararaman N, Morgera SD, Vertes RP (2007) Analysis of the actions of nucleus reuniens and the entorhinal cortex on EEG and evoked population behaviour of the hippocampus. *Conf Proc IEEE Eng Med Biol Soc* 2007:2480–2484



- Nettleton JS, Spain WJ (2000) Linear to supralinear summation of AMPA-mediated EPSPs in neocortical pyramidal neurons. *J Neurophysiol* 83:3310–3312
- Nunzi MG, Gorio A, Mila F, Freund TF, Somogyi P, Smith AD (1985) Cholecystinin-immunoreactive cells form symmetrical synaptic contacts with pyramidal and non-pyramidal neurons in the hippocampus. *J Comp Neurol* 237:485–505
- Paxinos G, Watson C (1986) *The rat brain in stereotaxic coordinates*, 2nd edn. Academic Press, Sydney
- Pereira de Vasconcelos A, Cassel JC (2015) The nonspecific thalamus: a place in a wedding bed for making memories last? *Neurosci Biobehav Rev* 54:175–196
- Pissadaki EK, Sidiropoulou K, Reczko M, Poirazi P (2010) Encoding of spatio-temporal input characteristics by a CA1 pyramidal neuron model. *PLoS Comput Biol* 6:e1001038
- Poirazi P, Brannon T, Mel BW (2003) Arithmetic of subthreshold synaptic summation in a model CA1 pyramidal cell. *Neuron* 37:977–987
- Prasad JA, Macgregor EM, Chudasama Y (2013) Lesions of the thalamic reuniens cause impulsive but not compulsive responses. *Brain Struct Funct* 218:85–96
- Prasad JA, Abela AR, Chudasama Y (2016) Midline thalamic reuniens lesions improve executive behaviors. *Neuroscience*
- Preston AR, Eichenbaum H (2013) Interplay of hippocampus and prefrontal cortex in memory. *Curr Biol* 23:R764–R773
- Price CJ, Cauli B, Kovacs ER, Kulik A, Lambollez B, Shigemoto R, Capogna M (2005) Neurogliaform neurons form a novel inhibitory network in the hippocampal CA1 area. *J Neurosci* 25:6775–6786
- Price JC, Scott R, Rusakov D, Capogna M (2008) GABA<sub>B</sub> receptor modulation of feed-forward inhibition through neurogliaform cells. *J Neurosci* 28:6974–6982
- Remondes M, Schuman EM (2002) Direct cortical input modulates plasticity and spiking in CA1 pyramidal neurons. *Nature* 416:736–740
- Remondes M, Schuman EM (2003) Molecular mechanisms contributing to long-lasting synaptic plasticity at the temporoammonic-CA1 synapse. *Learn Mem* 10:247–252
- Remondes M, Schuman EM (2004) Role for a cortical input to hippocampal area CA1 in the consolidation of long-term memory. *Nature* 431:699–703
- Roux L, Buzsáki G (2015) Tasks for inhibitory interneurons in intact brain circuits. *Neuropharmacology* 88:10–23
- Saalmann YB (2014) Intralaminar and medial thalamic influence on cortical synchrony, information transmission and cognition. *Front Syst Neurosci* 8:83. doi:10.3389/fnsys.2014.00083
- Samulack DD, Williams S, Lacaille J-C (1993) Hyperpolarizing synaptic potentials evoked in CA1 pyramidal cells by glutamate stimulation of interneurons from the oriens/alveus border of rat hippocampus slices. *Hippocampus* 3:331–344
- Schall KP, Kerber J, Dickson CT (2008) Rhythmic constraints on hippocampal processing: state and phase-related fluctuations of synaptic excitability during theta and slow oscillation. *J Neurophysiol* 99:888–899
- Sesack SR, Deutch AY, Roth RH, Bunney BS (1989) Topographical organization of the efferent projections of the medial prefrontal cortex in the rat: an anterograde track-tracing study with Phaseolus vulgaris leucoagglutinin. *J Comp Neurol* 290:213–242
- Sirota A, Buzsáki G (2005) Interactions between neocortical and hippocampal networks via slow oscillations. *Thalamus Relat Syst* 3:245–259
- Sirota A, Csicsvari J, Buhl D, Buzsáki G (2003) Communication between neocortex and hippocampus during sleep in rodents. *PNAS* 100:2065–2069
- Skelton RW, McNamara RK (1992) Bilateral knife cuts to the perforant path disrupt spatial learning in the Morris water maze. *Hippocampus* 2:73–80
- Sloviter RS (1991) Feedforward and feedback inhibition of hippocampal principal cell activity evoked by perforant path stimulation: GABA-mediated mechanisms that regulate excitability. *Hippocampus* 1:31–40
- Somogyi P, Klausberger T (2005) Defined types of cortical interneuron structure space and spike timing in the hippocampus. *J Physiol (Lond)* 562:9–26
- Somogyi P, Nunzi MG, Gorio A, Smith AD (1983) A new type of specific interneuron in the monkey hippocampus forming synapses exclusively with the axon initial segment of pyramidal cells. *Brain Res* 259:137–142
- Steward O (1976) Topographic organization of the projections from the entorhinal area to the hippocampal formation of the rat. *J Comp Neurol* 167:285–314
- Suh J, Rivest AJ, Nakashiba T, Tominaga T, Tonegawa S (2011) Entorhinal cortex layer III input to the hippocampus is crucial for temporal association memory. *Science* 334:1415–1420
- Swanson LW (1998) *Brain maps: structure of the rat brain*. 2. Elsevier Academic Press, San Diego
- Sybriska E, Davachi L, Goldman-Rakic PS (2000) Prominence of direct entorhinal-CA1 pathway activation in sensorimotor and cognitive tasks revealed by 2-DG functional mapping in nonhuman primate. *J Neurosci* 20:5827–5834
- Takács VT, Klausberger T, Somogyi P, Freund TF, Gulyás AI (2011) Extrinsic and local glutamatergic inputs of the rat hippocampal CA1 area differentially innervate pyramidal cells and interneurons. *Hippocampus* 22:1379–1391
- Takahashi H, Magee JC (2009) Pathway interactions and synaptic plasticity in the dendritic tuft regions of CA1 pyramidal cells. *Neuron* 62:102–111
- Takehara-Nishiuchi K (2014) Entorhinal cortex and consolidated memory. *Neurosci Res* 84:27–33
- Varela C, Kumar S, Yang JY, Wilson MA (2014) Anatomical substrates for direct interactions between hippocampus, medial prefrontal cortex, and the thalamic nucleus reuniens. *Brain Struct Funct* 219:911–929
- Vertes RP (2002) Analysis of projections from the medial prefrontal cortex to the thalamus in the rat, with emphasis on nucleus reuniens. *J Comp Neurol* 442:163–187
- Vertes RP, Hoover WB, Do Valle AC, Sherman A, Rodriguez JJ (2006) Efferent projections of reuniens and rhomboid nuclei of the thalamus in the rat. *J Comp Neurol* 499:768–796
- Vertes RP, Hoover WB, Szigeti-Buck K, Leranath C (2007) Nucleus reuniens of the midline thalamus: link between the medial prefrontal cortex and the hippocampus. *Brain Res Bull* 71:601–609
- Vida I, Halasy K, Szinyei C, Somogyi P, Buhl EH (1998) Unitary IPSPs evoked by interneurons at the stratum radiatum-stratum lacunosum-moleculare border in the CA1 area of the rat hippocampus in vitro. *J Physiol* 506:755–773
- Wang SH, Morris RG (2010) Hippocampal-neocortical interactions in memory formation, consolidation, and reconsolidation. *Annu Rev Psychol* 61:49–79
- Wei DS, Mei YA, Bagal A, Kao JP, Thompson SM, Tang CM (2001) Compartmentalized and binary behavior of terminal dendrites in hippocampal pyramidal neurons. *Science* 293:2272–2275
- Wheeler AL, Teixeira CM, Wang AH, Xiong X, Kovacevic N, Lerch JP, McIntosh AR, Parkinson J, Frankland PW (2013) Identification of a functional connectome for long-term fear memory in mice. *PLoS Comput Biol* 9:e1002853. doi:10.1371/journal.pcbi.1002853

- Wilson DIG, Watanabe S, Milner H, Ainge JA (2013) Lateral entorhinal cortex is necessary for associative but not nonassociative recognition memory. *Hippocampus* 23:1280–1290
- Witter MP, Griffioen AW, Jorritsma-Byham B, Krijnen JLM (1988) Entorhinal projections to the hippocampal CA1 region in the rat: an underestimated pathway. *Neurosci Lett* 85:193–198
- Wolansky T, Clement EA, Peters SR, Palczak MA, Dickson CT (2006) Hippocampal slow oscillation: a novel EEG state and its coordination with ongoing neocortical activity. *J Neurosci* 26:6213–6229
- Wouterlood FG (1991) Innervation of entorhinal principal cells by neurons of the nucleus reuniens thalami. Anterograde PHA-L tracing combined with retrograde fluorescent tracing and intracellular injection with Lucifer yellow in the rat. *Eur J Neurosci* 3:641–647
- Wouterlood FG, Saldana E, Witter MP (1990) Projections from the nucleus reuniens thalami to the hippocampal region: light and electron microscopic tracing study in the rat with the anterograde tracer Phaseolus vulgaris-leucoagglutinin. *J Comp Neurol* 296:179–203
- Wouterlood FG, Aliane V, Boekel AJ, Hur EE, Zaborsky L, Barros-Chinea P, Härtig W, Lanciego JL, Witter MP (2008) Origin of calretinin-containing, vesicular glutamate transporter 2-coexpressing fiber terminals in the entorhinal cortex of the rat. *J Comp Neurol* 506:359–370
- Xu W, Südhof TC (2013) A neural circuit for memory specificity and generalization. *Science* 339:1290–1295
- Zhang DX, Bertram EH (2002) Midline thalamic region: wide spread excitatory input to the entorhinal cortex and amygdala. *J Neurosci* 22:3277–3284
- Zhang Y, Yoshida T, Katz DB, Lisman JE (2012) NMDAR antagonist action in thalamus imposes delta oscillations on the hippocampus. *J Neurophysiol* 107:3181–3189